

РОЗСИЮВАННЯ І ДИФРАКЦІЯ ХВИЛЬ

SCATTERING AND DIFFRACTION OF WAVES

DOI: <https://doi.org/10.15407/rpra27.02.083>

УДК 621.396.67

PACS number: 84.40.Ba

L.M. Lytvynenko¹, S.A. Pogarsky², and D.V. Mayboroda²

¹ Institute of Radio Astronomy National Academy of Sciences of Ukraine

4, Mystetstv St., Kharkiv, 61002, Ukraine

² V.N. Karazin Kharkiv National University

4, Svobody Sq., Kharkiv, 61022, Ukraine

E-mail: spogarsky@gmail.com

ANALYSIS AND OPTIMIZATION OF THE OPERATING RANGE OF A MONOPOLE ANTENNA INVOLVING 'MEANDER' TYPE SLOT INHOMOGENEITIES

Subject and Purpose. The paper presents results of numerical modeling and experimental studies of a disk-shaped microstrip antenna involving 'meander' type slotted inhomogeneities. The work has been aimed at optimizing the operating range of the antenna and matching it to external circuits through the use of additional structural elements and appropriate feeding techniques.

Methods and Methodology. The design features a circular disk-shaped microstrip resonator containing within its plane groups of slotted inhomogeneities which form a segmented meander line, with the segments oriented relative one another at an angle of 120°. The antenna could be fed through a segment of a screened coplanar line. The location of the screening plane of the coplanar line, as well as its dimensions, were variable. Numerical simulation was carried out within the 'semi-open resonator' technique using the finite element method. The degree of optimization of the operating range was estimated, based on analyzing spectral characteristics of the antenna, for a variety of its geometric parameters, and the magnitude of the return loss over a given frequency range. Measurements of the VSWR were carried out with reflectometers.

Results. Frequency and power characteristics of a monopole, disk-shaped microstrip antenna have been analyzed and optimized over a wide frequency range. Mechanical dimensions of the additional shielding plane and location thereof have been identified as factors having significant influence upon the frequency-dependent, polarizational and power characteristics of the antenna.

Conclusions. The operating frequency range, spectral and power characteristics of a monopole, disk-shaped microstrip antenna have been studied both theoretically and experimentally. Numerical simulations were carried out with the use of the finite element method. Experimental studies of the frequency characteristics were performed using reflectometry techniques. The antenna considered can find practical application over a wide frequency range, either as a single radiating element in a device or system, or a constituent part of an antenna array.

Keywords: circular disk, slot, meander, coplanar line, radiation pattern.

Citation: Lytvynenko, L.M., Pogarsky, S.A., and Mayboroda, D.V., 2022. Analysis and Optimization of the Operating Range of a Monopole Antenna Involving 'Meander' Type Slot Inhomogeneities. *Radio Physics and Radio Astronomy*, 27(2), pp. 83–92. <https://doi.org/10.15407/rpra27.02.083>

Ц и т у в а н н я: Литвиненко Л.М., Погарський С.О., Майборода Д.В. Дослідження та оптимізація робочого діапазону монопольної антени, що містить щілинні неоднорідності типу меандра. *Радіофізика і радіоастрономія*. 2022. Т. 27. № 2. С. 83–92. <https://doi.org/10.15407/rpra27.02.083>

© Publisher PH "Akademperiodyka" of the NAS of Ukraine, 2022. This is an open access article under the CC BY-NC-ND license (<https://creativecommons.org/licenses/by-nc-nd/4.0/>)

© Видавець ВД «Академперіодика» НАН України, 2022. Статтю опубліковано відповідно до умов відкритого доступу за ліцензією CC BY-NC-ND (<https://creativecommons.org/licenses/by-nc-nd/4.0/>)

Introduction

Modern portable telecommunication devices such as mobile phones, tablets, GPS navigators, etc. combine a variety of wireless modules. The main trends in the development of such devices are to reduce their size and improve functionality [1, 2]. One of the most important elements of any telecommunication device is its antenna system. The trend toward miniaturization ultimately results in a situation where barely enough space is left for placing an antenna. This, inevitably, entails a noticeable deterioration of radiation parameters, the typical manifestations being low gain, distorted radiation pattern, decrease in efficiency, and reduced operating frequency band.

The introduction of new communication standards and exploration of new frequency ranges impose new requirements to such devices, namely, ability to operate in a multifrequency mode, while providing a sufficiently wide bandwidth of operating frequencies.

Many of these requirements can be met by microstrip antennas. Their main advantages include low profile; light weight; ability to work with waves of arbitrary polarization; a fairly simple integration into power supply circuits of antenna arrays, low cost and ease of implementation. But, despite all the advantages, they retain the disadvantage of a narrow relative bandwidth [3, 4].

The solution to the issue of expanding the operating frequency band is constantly at the center of attention of specialists in the field of microwave technology. Among the methods most frequently used for expanding the operating band, note the following:

The first, and practically the principal one, is to change the geometry and layout of the radiating aperture. As a result of increasing its length, the operating range can be shifted toward lower frequencies and degeneracy of a number of natural oscillations removed. Thus, the writers paper [5] presented data on a microstrip antenna involving a microstrip disk of a certain diameter, plus an annular microstrip conductor which was electrically coupled to the microstrip disk. The antenna was excited by a coaxial line section through galvanic contact with the microstrip disk. In essence, the electrodynamic structure represented two coupled resonators. So, by changing the degree of coupling between the resonators, it was possible to control the operating fre-

quency band (expanding that up to 10 per cent of the central frequency). At the same time, the structure demonstrated a significant drawback, namely that the antenna could operate only at frequencies from a discrete set.

Another technical solution based on changes in the layout of the radiating aperture is presented in paper [6]. The design included a microstrip disk complemented by a set of radially arranged slot inhomogeneities. The antenna was excited through a segment of a microstrip line that had galvanic contact with the microstrip disk. The design provided a fairly high level of performance [6], but also showed quite significant drawbacks. First, if a structural version were used that involved an odd number of slot inhomogeneities (else, these were located asymmetrically relative to one another), then energy parameters of such antennas depended essentially on position of the electromagnetic power feed. Second, the designs with an even number of slot discontinuities and symmetrical mode of power input ensured a relatively high level of matching with external circuits, but only through a narrow frequency band. And, finally, the excitation method suggested could only provide for effective operation near the frequencies of those eigenmodes whose phase centers were located near the edge of the disk-shaped resonator.

Yet another possible way to expand the bandwidth and create opportunities for multifrequency operation is to use radiating apertures involving periodic sequences of inhomogeneities of the same type. These could be, for example, meander type inhomogeneities [7], with the antenna excited by a coaxial segment. The use of such elements made it possible, on the one hand, to form several frequency zones with an acceptable level of matching, while on the other, to achieve a higher level of broadbandness (in some areas reaching 25 per cent). At the same time, it is not possible to talk about a radical solution to the issue of broadbandness.

An alternative approach is to use additional structural elements that may directly affect the excited eigenmode spectrum (for example, short circuiting elements). The desired expansion of the operating range may occur due to removal of the eigenmode degeneracy. Thus, the authors of paper [8] described a microstrip antenna of complex design, specifically a composition of a microstrip disk of a certain diameter and a circular sector of a larger radius. The angu-

lar aperture of the sector was 90° . The structure was excited via a segment of a coaxial line. The point of input of electromagnetic power was displaced radially from the center of the smaller disk where a 'length shortener' was installed on the ground plane. The structure demonstrated expansion of the bandwidth up to 15 or 18 per cent of the central frequency, however basic parameters of such an antenna depended significantly on the magnitude of the sectorial angle and location of the power input point. Accordingly, any technical missteps in the manufacturing procedure could lead to unpredictable results in what concerns the operating range and the emission bandwidth.

The present work has been aimed at both theoretical and experimental study of the monopole microstrip antenna involving slot-like inhomogeneities of 'meander' type, with further optimization of its performance parameters.

1. Structure under study

We will consider a monopole microstrip antenna with a set of 'meander' type slot inhomogeneities, excited by a section of a coplanar line that is partially screened off on the back of its dielectric substrate. A schematic representation of the geometry and layout of the structure are shown in Fig. 1 and the dimensions listed in Table. The basic microstrip disk is of diameter $d = 35$ mm. The axes of the meander line segments are at angles of 120° relative one another. The substrate material was NELCO NY9220 dielectric characterized by a relative permittivity $\epsilon_r = 2.2$.

Searches for an optimum way to excite monopole microstrip antennas with various kinds of inhomogeneities have been carried out rather intensely for quite a time [9]. The approach that seems most promising as for expanding the operating range of such antennas is the method of excitation that employs different versions of coplanar line sections [10]. It is necessary to mention kind of a regularity noted in many of the previous results. By properly selecting parameter ratios it was possible to implement a multifrequency operation mode within any excitation technique employing a full ground plane. Still, the width of the operating frequency band always remained small and, generally, it was not possible to achieve a sufficiently broad end-to-end frequency band.

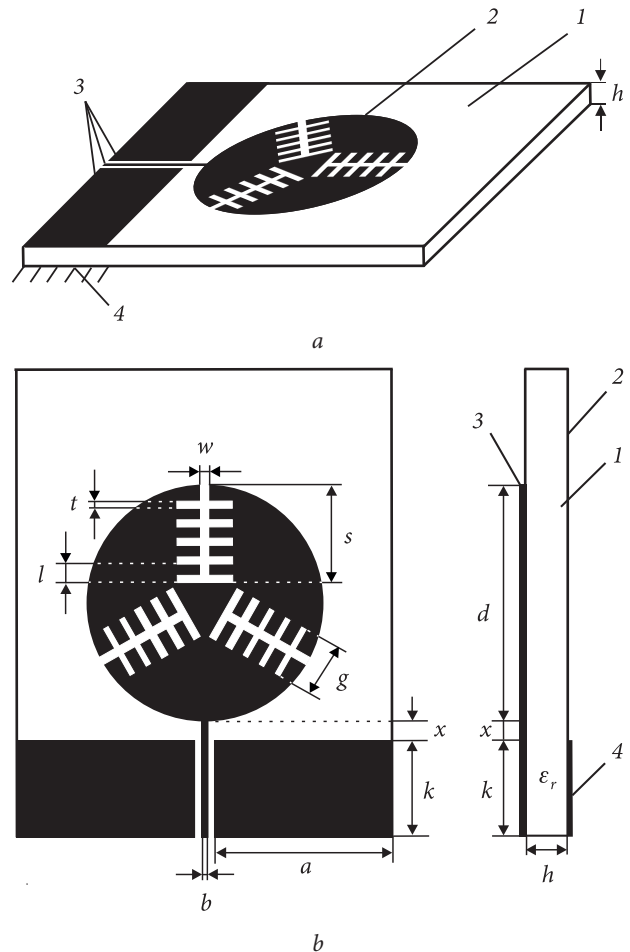


Fig. 1. Schematic representation, *a* and layout, *b* of the microstrip antenna under study

The main reason for such effects is that the presence of a screening plane determines the eigenmode spectrum in the structure, as well as the relative position of the eigenfrequencies on the frequency axis and the laws of power distribution in different parts of the structure (the major part concentrates in the substrate, between the ground plane and the plane of the disk). Ultimately, this affects all other electrodynamic and power parameters of the antennas. At the same time, with an optimal ratio of parameters, the shielding elements provide additional opportunities for controlling the antenna characteristics.

2. Simulation results

2.1. Structure matching

Parameters of the structures under consideration have been simulated within the 'semi-open resonator' model using the finite element method (FEM).

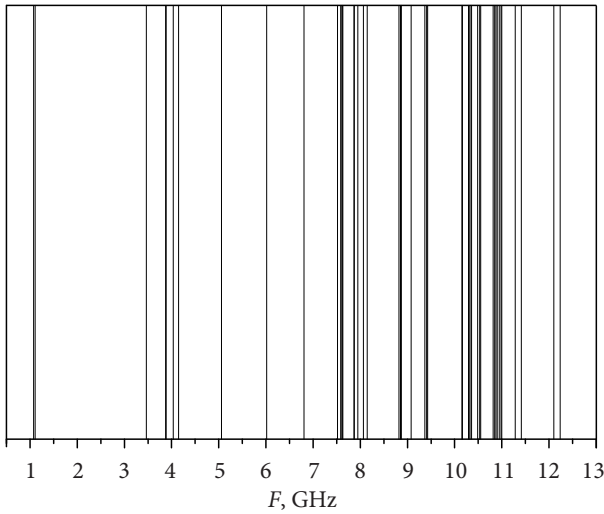


Fig. 2. Eigenfrequency spectrum of a fully screened microstrip structure

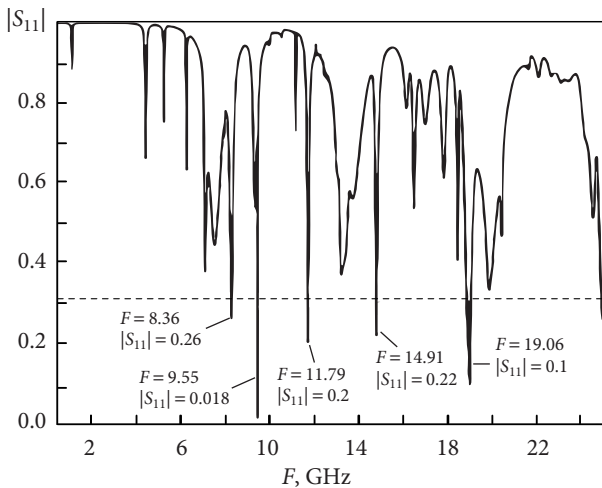


Fig. 3. Frequency dependence of $|S_{11}|$ (full shielding)

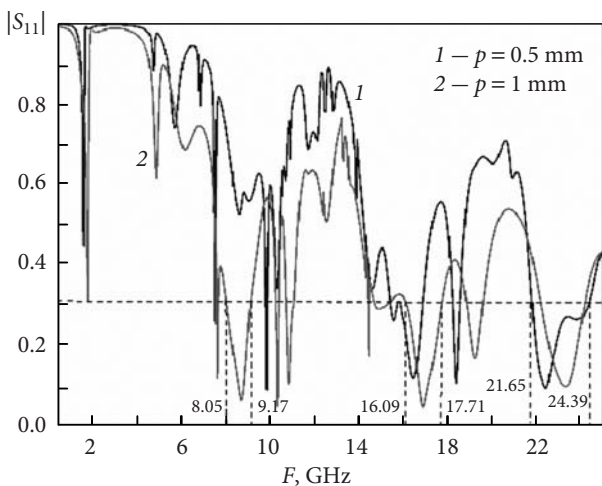


Fig. 4. Frequency dependence of $|S_{11}|$ in the case of full 'suspended' shielding'

Initially, some attempts were made to optimize the structure's parameters on the fully metallized back side of the substrate. It is known [11] that the so-called suspended lines of planar type, in which a ground plane is placed at a certain distance from the dielectric substrate, may offer some advantages when trying to expand the operating range. The variable selected as an optimization parameter was the size of the gap between the dielectric substrate and the ground plane. Some of the pertinent simulated results are shown in Figs. 2 and 3. Figure 2 presents the eigenmode spectrum of a structure in which the ground plane is located on the back side of the substrate (no air gap present). Calculations have shown that the presence of an air gap does not affect the number of oscillation modes excited. Moreover, it has practically no effect on their localization on the frequency axis (their shift toward the low-frequency part of the range never exceeded 0.005 per cent).

Analysis of the characteristics shows the distribution of the spectral lines to be extremely non-uniform. Two types of oscillations can be seen in a close vicinity of eigenfrequencies, specifically near $F \approx 1$ GHz (the separation between their frequencies is about 30 MHz). In the range from 3.5 GHz to 4.25 GHz, five eigenmodes are excited, and two degenerate modes are seen at $F = 3.87$ GHz. Only single modes are excited up to 7 GHz. At still higher frequencies more excitation ranges are observed, within which a significant number of oscillatory modes, including degenerate ones, are excited.

Figure 3 shows the frequency dependence of $|S_{11}|$ for a structure with a fully shielded back side of the substrate (no air gap). The dotted line shows the level corresponding to a return loss of -10 dB. The curve demonstrates sharp oscillations with prominent drops in the magnitude of $|S_{11}|$. Minima of $|S_{11}|$ are reached only at some of the frequencies (a multi-frequency mode can be realized), however the operating bands near these frequencies are very narrow (never exceeding fractions of one percent). Upon approaching to 19.08 GHz the band expands to a level of 1 per cent of the central frequency. By introducing a frequency gap between the dielectric substrate and the ground plane (setting $p \neq 0$) one can, to a certain degree, change the matching conditions. In Fig. 4 two dependences of $|S_{11}|$ upon frequency are shown for two values of the parameter p . Analysis of these dependences indicates that by introducing a

gap between the dielectric substrate and the ground plane it is possible to noticeably cut down the level of pulsations (especially in the high-frequency region). Also, the operating bands can be markedly expanded. In the vicinity of the spectral line $F = 8.75$ GHz, the operating bandwidth is $\Delta F = 1.12$ GHz with $p = 1$ mm (12.8 per cent of the central frequency). Near $F = 16.9$ GHz and with $p = 1$ mm, the operating bandwidth is $\Delta F = 1.63$ GHz (or 9.6 per cent of the central frequency). In the vicinity of $F = 22.98$ GHz and with a different value of p (namely, $p = 0.5$ mm), the bandwidth becomes $\Delta F = 2.74$ GHz (which is 11.9 per cent of the central frequency).

As follows from the above set of results, by applying 'full screening' alone it is hardly (if at all) possible to obtain wide end-to-end operating bands. Besides, sharp oscillations of $|S_{11}|$ over the frequency range cannot be excluded either. The physical reason is that the energy of the excited vibrations is concentrated within a very limited volume (at the same time, $p \ll \lambda_{res}$).

Another way to expand the operating range is to enlarge the virtual volume within which the oscillating power is concentrated [11]. That can be implemented by partially shielding the dielectric substrate. A conceptual change of the structure's geometry, like introduction of an air gap, certainly leads to a change in the spectral composition of oscillations and their location on the frequency axis. Shown in Fig. 5 are spectral characteristics of a structure with partial shielding and presence of an air gap (parameter $p = 0.5$ mm). The distance from the aperture of the basic disk to lateral conductors of the coplanar line (and the earthed part of the structure) was chosen in the course of optimization and equaled $x = 1.25$ mm. Comparison of the dependences presented in Fig. 2 and Fig. 5 shows that in the case of partial shielding, the most noticeable changes occur at frequencies below 8 GHz. Over the range from 0.5 GHz to 8 GHz, the spectral lines are distributed rather uniformly, which suggests a possibility of exciting a larger number of eigenmodes. Figure 6 shows the frequency dependence for a partially shielded dielectric substrate parameter and a fixed value of $p = 0$ mm.

As is evident from the dependences described, the use of partial shielding made it possible to obtain three fairly wide operating frequency bands, specifically between 4.43 GHz and 8.28 GHz (bandwidth $\Delta F = 3.85$ GHz, or 61 per cent of the central frequency

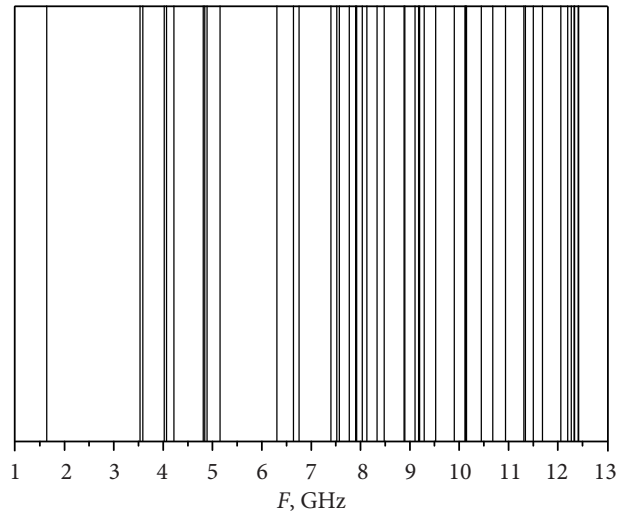


Fig. 5. Eigenfrequency spectrum of a partially shielded structure

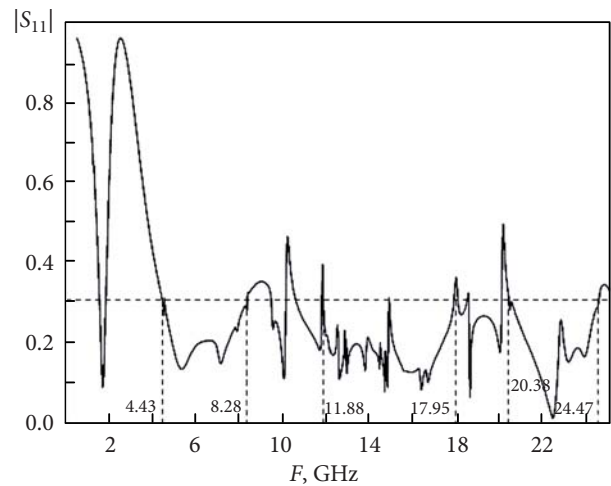


Fig. 6. Frequency dependence of $|S_{11}|$ (partial shielding, $p = 0$)

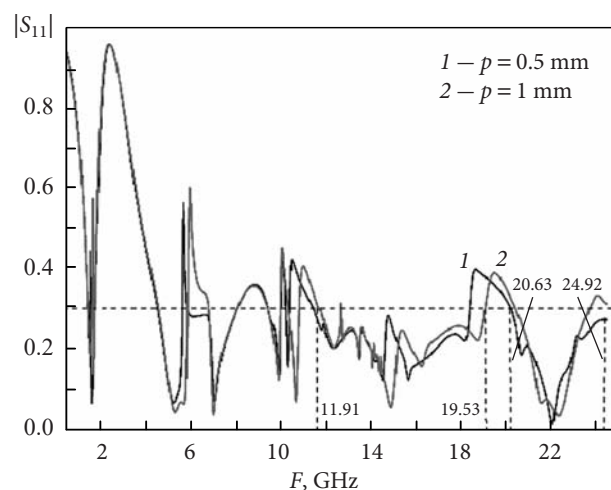


Fig. 7. Frequency dependences of $|S_{11}|$ with two values of the parameter p

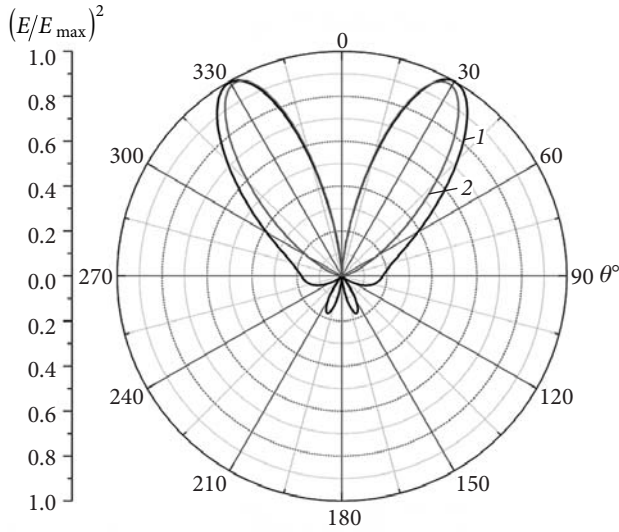


Fig. 8. Radiation patterns of a fully shielded structure (two values of the parameter p)

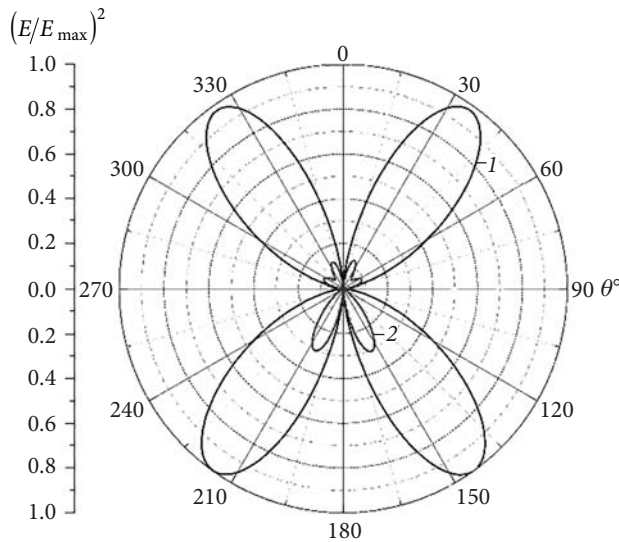


Fig. 9. Radiation patterns in the case of partial shielding (two values of the parameter p), with $k = 11.87$ mm

cy); between 11.88 GHz and 17.95 GHz (bandwidth $\Delta F = 6.07$ GHz, or 41% of the central frequency), and between 20.38 GHz and 24.47 GHz (an 18 per cent bandwidth). Figure 7 shows frequency dependences of $|S_{11}|$ for a variety of values of the parameter p . Evidently, introduction of a 1 mm wide air gap leads to disappearance of the first band, while the second one (between 11.91 GHz and 19.53 GHz) becomes noticeably more compact (of width $\Delta F = 7.62$ GHz, or 48 per cent of the central frequency). The third band reaches beyond the range under discussion, hence is not very promising from the point of impedance matching in a single-operation mode for the coplanar exciter.

2.2. Power characteristics

The formation of a certain (specified) spatial distribution of fields in the far zone, (and in some applications in the near-field zone as well), is the main task of any antenna system. In this regard, antenna structures with complex radiating apertures provide additional opportunities.

Figure 8 one presents radiation patterns of a structure with a 'meander' type, fully shielded aperture (two versions). In one of these the 'earthed' plane is located close to the dielectric substrate, $p = 0$ mm (curve 1). In the case of version two, the ground plane and the dielectric substrate are separated by an air gap $p = 1$ mm (curve 2).

The frequency $F = 8.37$ GHz was selected as the operating frequency. This choice is due to the proximity of this magnitude to one of the eigenfrequencies (see Fig. 2). As can be clearly seen, the radiation patterns consist of two lobes for both versions.

The appearance of the back radiation (full shielding) is explained by the fact that the structure is open in the directions of the OX and OY axes, so concentration of induced fields is possible on the reverse side of the metallized substrate.

Analysis of the dependences shows that in the absence of an air gap in the structure both lobes of the radiation pattern are oriented symmetrically relative the local normal. The directions of the lobe maxima are $\pm 30^\circ$ and width at the 3 dB level is $\sim 39.8^\circ$. The back lobes do not exceed -7.5 dB. With the introduction of an air gap ($p = 1$ mm), the pattern practically does not change, remaining two-lobed, as before. However, the lobe maxima now lie at $\pm 29^\circ$; the width at a 3 dB level has decreased to about $\sim 34^\circ$, while the level of back lobes has dropped down to -32.4 dB.

By 'shortening' the ground plane at the back side of the substrate (i.e., bringing its size to match the linear dimension of the coplanar transmission element, see Fig. 1, parameter $k = 11.87$ mm) one can achieve a noticeable change in the radiation pattern. Fig. 9 shows elevation-plane radiation patterns for two operating frequencies. Curve 1 corresponds to a frequency $F = 5.87$ GHz, while curve 2 to $F = 8.37$ GHz. These frequencies have been chosen because of their proximity to the corresponding spectral lines and an optimal value of $|S_{11}|$. All the dependences presented have been normalized to a global maximum.

The radiation patterns at both frequencies are multi-lobed. Moreover, the level of the radiated po-

wer at a lower frequency is about 5 times lower than at the higher one. The pattern at $F = 5.87$ GHz turns out to be four-lobed and almost symmetric about the center of the coordinate system. The field amplitudes in the directions of pattern maxima fluctuate insignificantly (not exceeding the levels of 2 or 3 per cent). The width of the lobes at the level of 3 dB is $\sim 41.6^\circ$. At the frequency of $F = 8.37$ GHz, the pattern has a more complex form: While remaining two-lobed in the lower half-plane, it demonstrates two additional interference lobes in the upper half-plane. Shown in Fig. 10 are two elevation-angle dependences of the ellipticity ratio. In the case of totally shielded back side of the substrate only linear polarization of the radiated fields was observed (the polarization coefficient fluctuated in the range of 40 to 100 dB, therefore the correspondent graphs are not shown). Following a 'truncation', alias shortening, of the grounding surface to $k = 11.87$ mm, significant changes occur in the pattern. Localized angular zones appear within which elliptically polarized radiation fields is ecome observable. Moreover, their ellipticity ratio may reach values of 0.41 to 0.47.

The introduction of an additional gap between the dielectric substrate and the shortened ground base changes fundamentally both the power and polarizational characteristics of the structure. In Fig. 11 one can find elevation-plane radiation patterns of a structure with a 'suspended' substrate. Curve 1 corresponds to the frequency $F = 5.87$ GHz, and curve 2 to $F = 8.37$ GHz. Both curves are normalized to the global maximum magnitude. Obviously, a significant redistribution of the radiated fields has occurred. Now the amplitude at $F = 5.87$ GHz is about 0.4 of the correspondent amplitudes at $F = 8.37$ GHz. At the frequency of $F = 5.87$ GHz, the pattern remains four-lobed, however, it becomes markedly asymmetric with respect to the plane which contains the emitting aperture. The radiation pattern for the frequency $F = 8.37$ GHz has undergone a noticeable deformation becoming three-lobed in the lower half-plane. Two of the lobes are located symmetrically about the center, at the angles of 228° and 132° , with roughly equal lobe widths, about 32.4° , at the 3 dB level. The third lobe which is oriented orthogonally to the plane of the emitting aperture, turns out to be of a shorter width, not exceeding 24° at the 3 dB level. In addition, there are three low-amplitude interference lobes in the upper half-plane of the aperture.

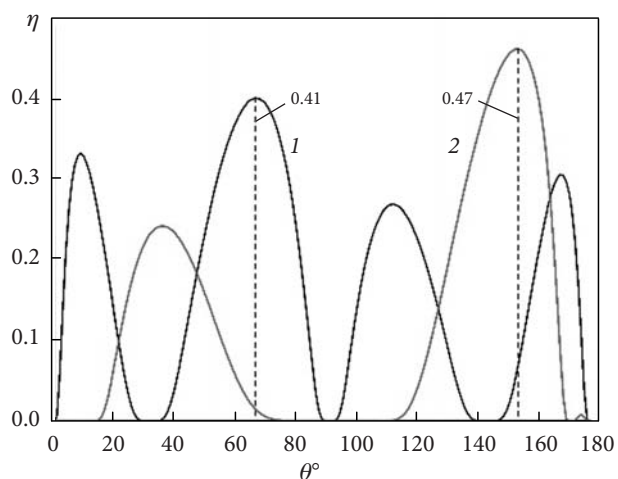


Fig. 10. Ellipticity ratio η versus elevation angle θ (deg)

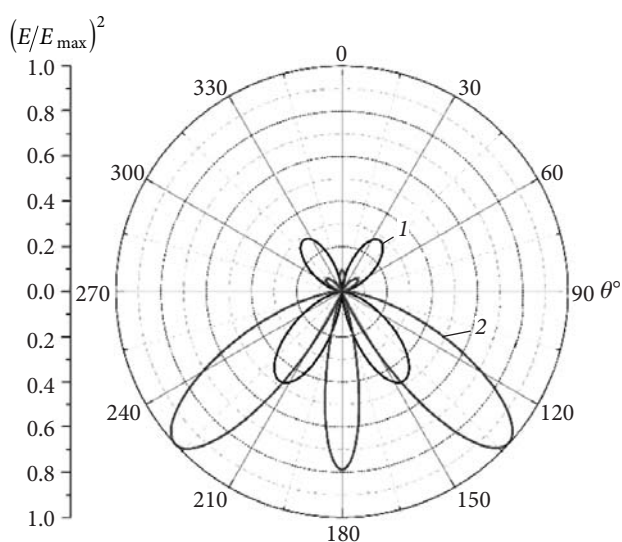


Fig. 11. Radiation patterns in the case of partial shielding (two values of p), with $k = 11.87$ mm and in presence of air gap

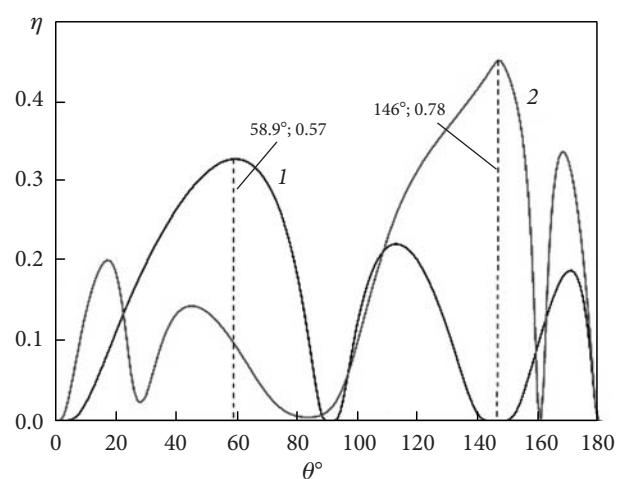


Fig. 12. Elevation angle dependences of the ellipticity ratio η

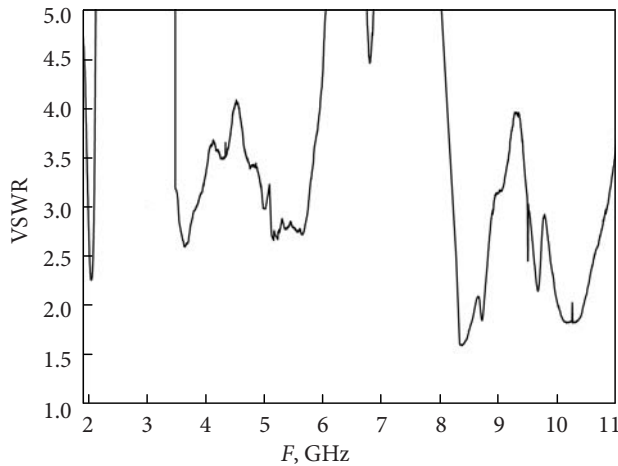


Fig. 13. Frequency dependence of the VSWR for a partially shielded structure ($k = 11.87$ mm)

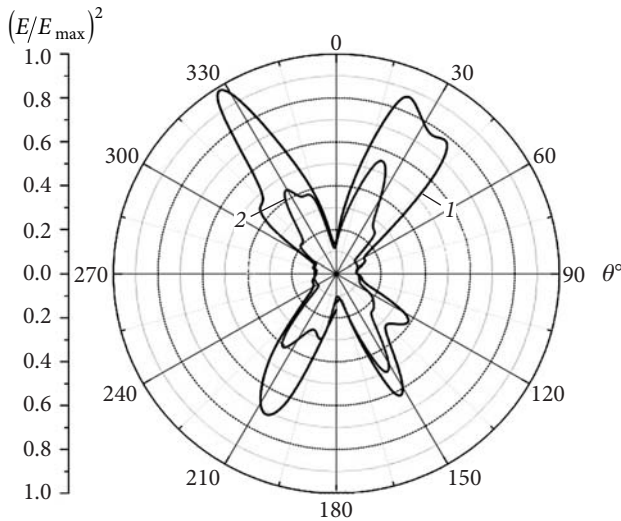


Fig. 14. Elevation-plane radiation patterns of a 'shortened' structure without an air gap

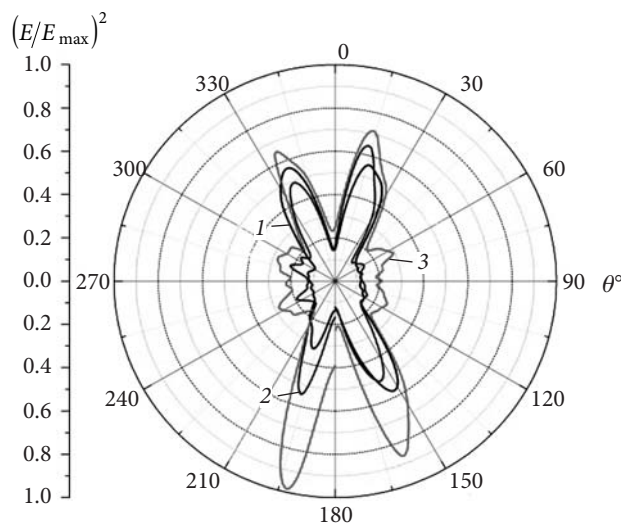


Fig. 15. Elevation-plane radiation patterns of a 'shortened' structure without an air gap

In Fig. 12 one can find the respective elevation-angle dependences for the ellipticity ratio. Both characteristics are fundamentally different from such of the fully shielded structure, also differing from the structure with partial shielding. Thus, at the frequency $F = 5.87$ GHz, one local angular strip, of width about 30° , is observed near the angle of 58.9° , within which the ellipticity ratio reaches a value like 0.57. Meanwhile, at $F = 8.37$ GHz the ellipticity ratio observable over a 60° interval near the angle 148° , turns out to be higher than 0.65, even reaching a maximum of 0.78.

3. Experimental results

Proceeding from the preliminary numerical results, a breadboard structure was prepared for measuring some spectral and power characteristics of an emitting module that would not involve an air gap between the dielectric substrate and the ground plane. Figure 13 presents the experimentally obtained frequency dependence of the VSWR in the radiating structure. In the experiment, an upgraded coaxial junction was used to excite the coplanar line.

Quite evidently, the measured VSWR is in excess of the 'threshold' value $VSWR = 2$, practically through the entire frequency range. An exception is the sub-range from 8.26 to 8.68 GHz, within which the VSWR turns out to be lower than the 'threshold' value.

If we focus on the theoretically obtained values (see Fig. 6), then we can talk about coincidence of frequency ranges with low VSWR values. Thus, in calculations for $F = 8.28$ GHz, the value of $|S_{11}| = 0.31$ corresponds to a $VSWR = 1.61$. In the experiment, the minimum value of $VSWR = 1.61$ was observed at a frequency of $F = 8.32$ GHz. The frequency offset is equal to 40 MHz, which is approximately 0.48 per cent of the central frequency. This frequency shift itself and the lower VSWR value can be explained by the fact that the complexity of the radiating structure's exciter (a coplanar segment, plus a coaxial junction) that was intended for ensuring sub-matching with external circuits, has not been taken into account in the numerical modeling.

To measure the power characteristics, the same frequencies were chosen at which the numerical simulation was carried out (namely, $F = 5.87$ GHz and $F = 8.37$ GHz).

Figure 14 presents radiation patterns at $F = 5.87$ GHz (curve 1) and at a close frequency of $F = 6.19$ GHz (curve 2). The latter frequency was se-

lected owing to its proximity to the frequency of a natural spectral line (see Fig. 2).

Both charts are normalized to the global maximum. Apparently, the pattern is two-lobed both in the upper and lower half-planes. Each of the lobes (except one) demonstrate more or less noticeable amplitude fluctuations.

Comparison of the measured and the numerically simulated dependences (cf. Fig. 9, curve 1 versus Fig. 14) reveals coincidence of both the radiation pattern forms and of the lobe orientations. The minimum difference in the corresponding angles is 2° , and the maximum is close to 8° . The highest degree of asymmetry in the shape of the lobes is noticeable from the side of power supply to the structure. Here, the coupling of the basic microstrip disk and the coplanar segment is most pronounced. Despite the relative proximity of the frequencies in the experiment (curve 1 and curve 2), the level of power radiated at 6.19 GHz is nearly by half lower (Fig. 14). Still, the shape of the pattern lobes is preserved almost completely.

In order to trace the dynamics of changes in the shape of the radiation pattern and the level of the radiated power, consider the radiation patterns shown in Fig. 15 for the frequency $F = 8.37$ GHz and several frequencies nearby. All three charts are normalized by the global maximum. Curve 1 corresponds to the frequency $F = 8.178$ GHz, curve 2 corresponds to $F = 8.37$ GHz, and curve 3 to $F = 8.93$ GHz.

Comparing the measured patterns of Fig. 15 with those obtained through numerical modeling we can note both a fairly good coincidence of parameters and the existence of certain differences. In the case of the simulated patterns the lobe maxima in the lower half-plane were oriented toward 153 and 208° . In the experiment, the pattern maxima were observed at the angular coordinates of 156 and 198° , showing amplitudes comparable to their respective values from the lower half-plane. The radiated field amplitude at $F = 8.93$ GHz demonstrated a significant increase, while the ratio of the radiated field amplitudes in the upper and lower half-planes practically did not change.

The physical interpretation of the results obtained can be as follows. In the first case (frequency $F = 5.87$ GHz), the value of $|S_{11}|$ does not exceed 0.17 (a $VSWR \approx 1.4$), i.e. the frequency belongs to a frequency range with a good level of matching. In the second case (frequency $F = 8.37$ GHz), the magnitude of $|S_{11}|$ reaches 0.31 (the correspondent value of $VSWR \approx 1.91$). This means that the frequency belongs to a particular subrange characterized by a satisfactory level of conformance. Moreover, it is near these frequencies that resonances can be observed, owing to specific values of the wavelength and parameter ratios. The presence of possible resonances increases the rigidity of requirements as for geometric dimension tolerances in the radiating structure elements, and hence for compliance with technical and manufacturing requirements.

Conclusions

The paper presents results of theoretical and experimental studies of a monopole microstrip antenna with slotted inhomogeneities of the 'meander' type. The antenna could be excited using a segment of a modernized coplanar line. In the course of research, it was found that one of the key elements of the antenna, specifically the earthed base plays a key role in optimizing the antenna parameters. A change in the structure and layout of the earthed base (e.g., 'shortening' to a pre-selected value) can lead not only to a change in the possible spectral composition of eigenmodes in the structure, but also to a significantly altered level of matching, formation of sufficiently wide frequency regions with low $VSWR$ values, and possibility of control over certain power characteristics. The use of so-called 'suspended' structural elements provides additional opportunities for optimizing antenna parameters.

Acknowledgment

This work was supported by the Ministry of Education and Science of Ukraine (Ref. 0118U002038, 0119U002535).

REFERENCES

1. Bukhori, M.F., Misran, N.N., Islam, M.T., Yunus, M.M., Shakib, M.N., 2008. Design of microstrip antenna GPS application. In: *2008 IEEE Int. RF and Microwave Conf. (RFM)*. Kuala Lumpur, Malaysia, 2–4 Dec. 2008. IEEE Publ., pp. 464–466. DOI: 10.1109/RFM.2008.4897468.
2. Leilei, Liu, Xiao, Shi and Yan, Zang, 2010. Consideration of UWB circular disk antenna miniaturization. In: *2010 IEEE. 12th Int. Conf. Communication Technology (ICCT)*. Nanjing, China, 11–14 Nov. 2010. IEEE Publ., pp. 1141–1144. DOI: 10.1109/ICCT.2010.5689148.
3. Lo, Y.T., Solomon, D. and Richards, W.F., 1979. Theory and Experiment on Microstrip Antennas. *IEEE Trans. Antennas Propag.*, 27(2), pp. 137–145. DOI: 10.1109/TAP.1979.1142057.
4. Kin-Lu, Wong, 2002. *Compact and Broadband Microstrip Antennas*. John Wiley & Sons. DOI: 10.1002/0471221112.
5. Hall, P.S. and Prior, C.J., 1991. *Improvements in or relating to microstrip antennas*. EP. Pat. 0174068B1. Available at: <https://patents.google.com/patent/EP0174068B1/en>.
6. Maiboroda, D.V. and Pogarsky, S.A., 2014. On the choice of optimal topology of a reflecting module based upon the circular microstrip structure. *Telecommunication and Radio Engineering*, 73(19), pp. 1713–1726. DOI: 10.1615/TelecomRadEng.v73.i19.20.
7. Mayboroda, D.V., 2015. Microstrip disk antenna with complicated radiators. *Telecommunication and Radio Engineering*, 74(20), pp. 1777–1782. DOI: 10.1615/TelecomRadEng.v74.i20.10.
8. Conroy, P.J. and Ariz, S., 1977. *Broadband microstrip disc antenna*. US. Pat. 4160976. Available at: <https://patents.google.com/patent/US4160976?oq=usa+4160976>.
9. Pogarsky, S.A., Lytvynenko, L.M., Mayboroda, D.V. and Poznyakov, A.V., 2018. Influence of excitation method on the integral characteristics of circular patch monopole antennas. *Telecommunications and Radio Engineering*, 77(17), pp. 1485–1495. DOI: 10.1615/TelecomRadEng.v77.i17.10.
10. Swathi, A., Pavithra, J.J., Divya, S., Indhumathi, V., Suganthi, S. and Raghavan, S., 2013. A novel ANN optimized CPW fed truncated star shaped fractal antenna for wireless applications. *Int. J. Microwaves Appl.*, 2(2), pp. 77–84. Available at: <http://warse.org/pdfs/2013/ijma07222013.pdf>.
11. Kumar, G. and Ray, K.P., 2003. *Broadband microstrip antennas*. Artech House. Available at: <http://read.pudn.com/downloads150/ebook/652719/Broadband%20microstrip%20antennas.pdf>.

Received 25.04.22

L.M. Литвиненко¹, С.О. Погарський², Д.В. Майборода²

¹ Радіоастрономічний інститут НАН України
4, вул. Мистецтв, Харків, 61002, Україна

² Харківський національний університет імені В.Н. Каразіна
4, майдан Свободи, Харків, 61022, Україна

ДОСЛІДЖЕННЯ ТА ОПТИМІЗАЦІЯ РОБОЧОГО
ДІАПАЗОНУ МОНОПОЛЬНОЇ АНТЕНИ, ЩО МІСТИТЬ
ЩІЛИННІ НЕОДНОРІДНОСТІ ТИПУ «МЕАНДР»

Предмет і мета роботи. У роботі представлено результати чисельного моделювання та експериментальних досліджень мікросмужкової антени дискової геометрії, що містить щілинні неоднорідності типу «меандр». Метою роботи є оптимізація робочого діапазону антени та її узгодження із зовнішніми колами за рахунок використання додаткових конструктивних елементів і способів збудження.

Методи та методологія. Основою конструкції антени є кільцевий дисковий мікросмужковий резонатор, у площині якого містяться групи щілинних неоднорідностей, що утворюють відрізки меандрової лінії, орієнтовані один відносно одного під кутом 120°. Збудження антени здійснювалося за допомогою відрізка екранованої компланарної лінії. Місце розташування плоского екрана компланарної лінії та його розміри були варіативними. Чисельне моделювання виконано в техніці напіввідкритого резонатора за допомогою методу скінченних елементів. Ступінь оптимізації робочого діапазону оцінено на основі аналізу спектральної характеристики антени при варіації її геометричних параметрів та аналізу величини зворотних втрат у заданому частотному діапазоні. Експериментальні вимірювання величини КСХН здійснено з використанням рефлектометричних методів.

Результати. Проаналізовано й оптимізовано частотні та енергетичні характеристики монопольної дискової мікросмужкової антени в широкому частотному діапазоні. Виявлено фактор суттєвого впливу геометричних розмірів і місця розташування додаткового плоского екрана на частотні, поляризаційні та енергетичні характеристики антени.

Висновки. Теоретично й експериментально досліджено частотні, спектральні та енергетичні характеристики монопольної дискової мікросмужкової антени. Чисельне моделювання здійснено за допомогою методу скінченних елементів. Експериментальне дослідження частотних характеристик проведено з використанням рефлектометра. Антена може знайти практичне застосування в широкому діапазоні частот як поодинокій випромінювач у пристроях або системах, так і складовий елемент антенних решіток.

Ключові слова: круговий диск, щілина, меандр, компланарна лінія, діаграма направленості.